Chemical Science

Accepted Manuscript

This article can be cited before page numbers have been issued, to do this please use: J. Lin, S. Chen, K. Peng, Y. Hsu, S. Li, L. Cui, H. Zhang, Y. Wang, X. F. Lu, S. Wang, K. Liu, S. Hung and X. Wang, *Chem. Sci.*, 2026, DOI: 10.1039/D6SC02736A.




ROYAL SOCIETY OF CHEMISTRY

rsc.li/chemical-science

View Article Online
DOI: 10.1039/D6SC02736A

ARTICLE

# Photo-driven transient frustrated Lewis pairs for catalytic hydrogenation

Received 00th January 20xx,
Accepted 00th January 20xx

DOI: 10.1039/x0xx00000x

Jin Lin,[a] Shuanghui Chen,[a] Kang-Shun Peng,[b] Yung-Hsi Hsu,[b] Shuchun Li,[a] Longji Cui,[a] Hansong Zhang,[c] Yongjie Wang,[c] Xue Feng Lu,[a] Sibo Wang,[a] Kunlong Liu,[a,*] Sung-Fu Hung,[b,d,*] and Xinchen Wang [a,*]

Heterogeneous frustrated Lewis pairs (FLPs) have emerged as an effective strategy to transform catalytically inert support into active sites for hydrogenation reactions. However, the practical application of FLP sites remains limited due to their random spatial distribution and limited capacity to activate $H_2$. To address these challenges, we report the rational design of a highly effective FLP-based catalysts by anchoring isolated Rh atoms onto the $CeO_2$, achieving a hydrogenation rate of 35%/h for styrene, remarkedly outperforming pristine $CeO_2$ (2.74%/h). It is found that Rh species on $CeO_2$ form interfacial Rh-O-Ce sites, which play a critical role in the heterolytic cleavage of $H_2$ into Rh-$H^{\delta-}$ and O-$H^{\delta+}$ species. Upon light irradiation, the hydrogen spillover process is significantly promoted, enabling more efficient migration of activated hydrogen species to FLP sites and thereby facilitating $H_2$ dissociation under mild conditions. Moreover, photoexcitation of $CeO_2$ generates abundant transient FLPs on the surface, which serve as additional active sites for hydrogenation, leading to a substantial enhancement in photocatalytic activity. Similar synergistic effects are also observed when other semiconductor supports are employed, indicating the generality of this strategy. These findings provide a new strategy for designing synergistic dual-active-site systems that integrate interfacial metal-oxide sites with photoinduced FLPs for efficient photocatalytic hydrogenation reactions.

## Introduction

Heterogeneous frustrated Lewis pairs (FLPs) can effectively activate and transform small molecules through strong orbital interactions between FLP sites and reactant molecules, thereby converting catalytically inert oxides into active catalytic platform.[1-3] Despite substantial progress in heterogeneous FLP catalysis, their practical applications remain limited, mainly due to the random spatial distribution and inevitable agglomeration of FLP sites.[4-7] Fortunately, the introduction of oxygen vacancies ($V_O$s) into oxide supports not only enhances the acidity of Lewis acidic sites but also strengthens the basicity of the corresponding Lewis base sites. This dual modulation significantly improves the catalytic performance of heterogeneous FLPs.[8-10] However, although various strategies have been developed to generate oxygen vacancies on inert oxide surfaces, the precise construction and regulation of FLP sites via $O_V$ engineering remain a formidable challenge.[11]

In photocatalysis, efficient charge separation can induce transient rearrangements of the electronic structure within photocatalysts.[12, 13] Photogenerated electron-hole pairs preferentially accumulate at different atomic sites—photogenerated holes locally decrease electron density, generating transient Lewis acid sites,[14-16] whereas photogenerated electrons enrich electron density at neighboring sites, forming transient Lewis base or Lewis acid-base pairs.[17-19] Accordingly, rational photocatalyst design offers a promising route for precise and dynamic construction of FLP sites under light irradiation.

FLP catalytic systems. composed of sterically hindered electron donors and receptors, represent one of the most successful classes of emerging hydrogenation catalysts.[20-22] However, $H_2$ dissociation over heterogeneous FLPs is often hindered by their electronic structure, and as a result, most reported FLP-mediated hydrogenation reactions require harsh reaction conditions. In this context, decorating highly reactive metals (e.g., Rh, Pd) as atomically dispersed sites on oxide matrices has been emerged as an effective strategy to enhance hydrogenation activity.[23-25] The resulting metal-O-Ce interfacial structures can heterolytically activate $H_2$ into metal-$H^{\delta-}$ and O-$H^{\delta+}$ species, which subsequently migrate onto the oxide surface where hydrogen addition occurs via a hydrogen spillover process.[7, 26-28] By physically decoupling $H_2$ activation and hydrogenation sites, hydrogen spillover offers a unique

[a] State Key Laboratory of Chemistry for NBC Hazards Protection, State Key Laboratory of Photocatalysis on Energy and Environment, College of Chemistry, Fuzhou University, Fuzhou 350116, China.
[b] Department of Applied Chemistry and Center for Emergent Functional Matter Science, National Yang Ming Chiao Tung University, Hsinchu 300, Taiwan
[c] Guangdong Provincial Key Laboratory of Semiconductor Optoelectronic Materials and Intelligent Photonic Systems, School of Integrated Circuits, Harbin Institute of Technology, Shenzhen 518051, China.
[d] Department of Medicinal and Applied Chemistry, Kaohsiung Medical University, Kaohsiung 807, Taiwan.
†Corresponding authors: Email: klliu@fzu.edu.cn, sungfuhung@nycu.edu.tw, xcwang@fzu.edu.cn

View Article Online
DOI: 10.1039/D6SC02736A



opportunity to activate heterogeneous FLPs for efficient catalytic hydrogenation.[29-31] On this basis, we reason that semiconductor-supported single atom catalysts can further benefit from the synergistic effects of hydrogen spillover and light irradiation, enabling enhanced catalytic hydrogenation under mild conditions.

In this work, we demonstrate that anchoring isolated Rh atoms onto $CeO_2$ effectively overcomes the intrinsic limitations of heterogeneous FLPs, thereby significantly enhancing the photocatalytic hydrogenation performance of $CeO_2$ under mild conditions. The resulting $Rh_1/CeO_2$ catalyst readily transforms catalytically inert FLP sites into highly active hydrogenation centers and exhibiting a substantially higher photocatalytic activity for styrene hydrogenation compared with pristine $CeO_2$. Mechanistic investigations reveal that isolated Rh species form interfacial Rh-O-Ce sites, which are responsible for the heterolytic activation of $H_2$. Under light irradiation, two cooperative effects are observed: (i) photo-enhanced hydrogen spillover facilitates the migration of activated H species from Rh-O-Ce interfaces to FLP sites on $CeO_2$, and (ii) photoexcitation of $CeO_2$ generates a high density of transient surface FLPs. The synergistic interplay between these two photoinduced processes significantly improves both the activity and stability of photocatalytic hydrogenation. Notably, similar synergistic effects are also observed when other semiconductor supports are employed, indicating the generality of this strategy. This study establishes a synergistic dual-active-site concept—integrating interfacial metal-oxide sites with photoinduced FLPs—as an effective and broadly applicable approach for enhancing photocatalytic hydrogenation reactions.

## Results and discussion

The model $CeO_2$ photocatalyst used in this study was synthesized via the hydrothermal method (Figure S1).[32] Isolated Rh species was subsequently deposited onto the as-prepared $CeO_2$, using NaOH as the precipitating agent, yielding the $Rh_1/CeO_2$ catalyst.[33] As shown in Figure 1a and Figure S2, high-angle annular dark-field scanning transmission electron microscopy (HAADF-STEM) images clearly confirm the atomic dispersion of Rh species on the fresh $Rh_1/CeO_2$ catalyst, with no evidence of Rh nanoparticles formation (Figure S3). The atomic dispersion of Rh was further corroborated by *in situ* FTIR spectroscopy following CO pre-adsorption (Figure S4). Only characteristic symmetric and asymmetric stretching vibrations of $Rh(CO)_2^{+1}$ gem-dicarbonyl species were observed at around 2070 and 2000 $cm^{-1}$, respectively, indicating the presence of isolated Rh sites.[34] The local coordination environment of Rh atoms was further elucidated by X-ray absorption spectroscopy (XAS) measurements (Figures 1b,c; Figures S5-7, 10; Table S1). Wavelet transform (WT) contour plots of the Rh K-edge exhibit a single dominant feature at 5.5 $Å^{-1}$, which can be assigned to Rh-O scattering. Notably, no Rh-Rh contributions were detected in either the WT or Fourier-transformed (FT) extended X-ray absorption fine-structure analysis EXAFS spectra. Quantitative EXAFS fitting reveals a Rh-O coordination number close to four, further confirming the absence of Rh-Rh interaction (Figure S7 and Table S1).

$CeO_2$-based catalysts are well documented to be effective for alkene hydrogenation. Accordingly, styrene hydrogenation was selected as a model reaction to evaluate both the photocatalytic and thermocatalytic performance of $Rh_1/CeO_2$. As illustrated in Figure 1d and Figures S8-9, incorporation of isolated Rh species leads to a clear enhancement in catalytic activity compared with pristine $CeO_2$; however, under dark conditions the activity remains relatively limited. Remarkably, upon light irradiation, the $Rh_1/CeO_2$ catalyst exhibits a pronounced enhancement in both activity and stability, achieving 100% styrene conversion within 3 hours at a Rh:styrene molar ratio of 1:1000. This performance is approximately three times higher than the observed under dark conditions. Moreover, the catalyst maintains high activity over seven consecutive reaction cycles without noticeable deactivation (Figure 1e), demonstrating excellent durability during photocatalytic hydrogenation. CO adsorption measurements conducted after cycling confirm that Rh species remain atomically dispersed, indicating the structural robustness of the $Rh_1/CeO_2$ catalyst (Figure S11). Collectively, these results demonstrate that light irradiation plays a critical role in enhancing the hydrogenation performance of semiconductor-based catalysts.

Given that the $Rh_1/CeO_2$ catalyst contains two potential hydrogenation sites—Rh-O-Ce interfacial sites and FLPs sites on $CeO_2$—we next evaluate the individual catalytic contributions of these sites prior to mechanistic analysis of the photo-enhanced effect. As shown in Figure 1f and Figures S12 and S13, the Rh loading was systematically varied to investigate the role of Rh-O-Ce interfacial sites. Although decreasing Rh loading leads to a reduction in overall catalytic activity, the decrease is notably non-linear. Specifically, when the Rh loading is reduced from 0.2 wt% to 0.025 wt% (Table S2), the catalytic activity does not decrease proportionally; instead, 71.65% of the activity observed at 0.20 wt% Rh is retained. This behavior indicates a substantial contribution from the $CeO_2$ support to the hydrogenation process. Considering that pristine $CeO_2$ is unable to efficiently activate $H_2$ under mild conditions, the high hydrogenation activity of $Rh_1/CeO_2$ is predominantly attributed to hydrogen spillover, wherein H species activated at Rh-O-Ce interfacial sites migrate onto the $CeO_2$ surface and participate in subsequent hydrogenation reactions.

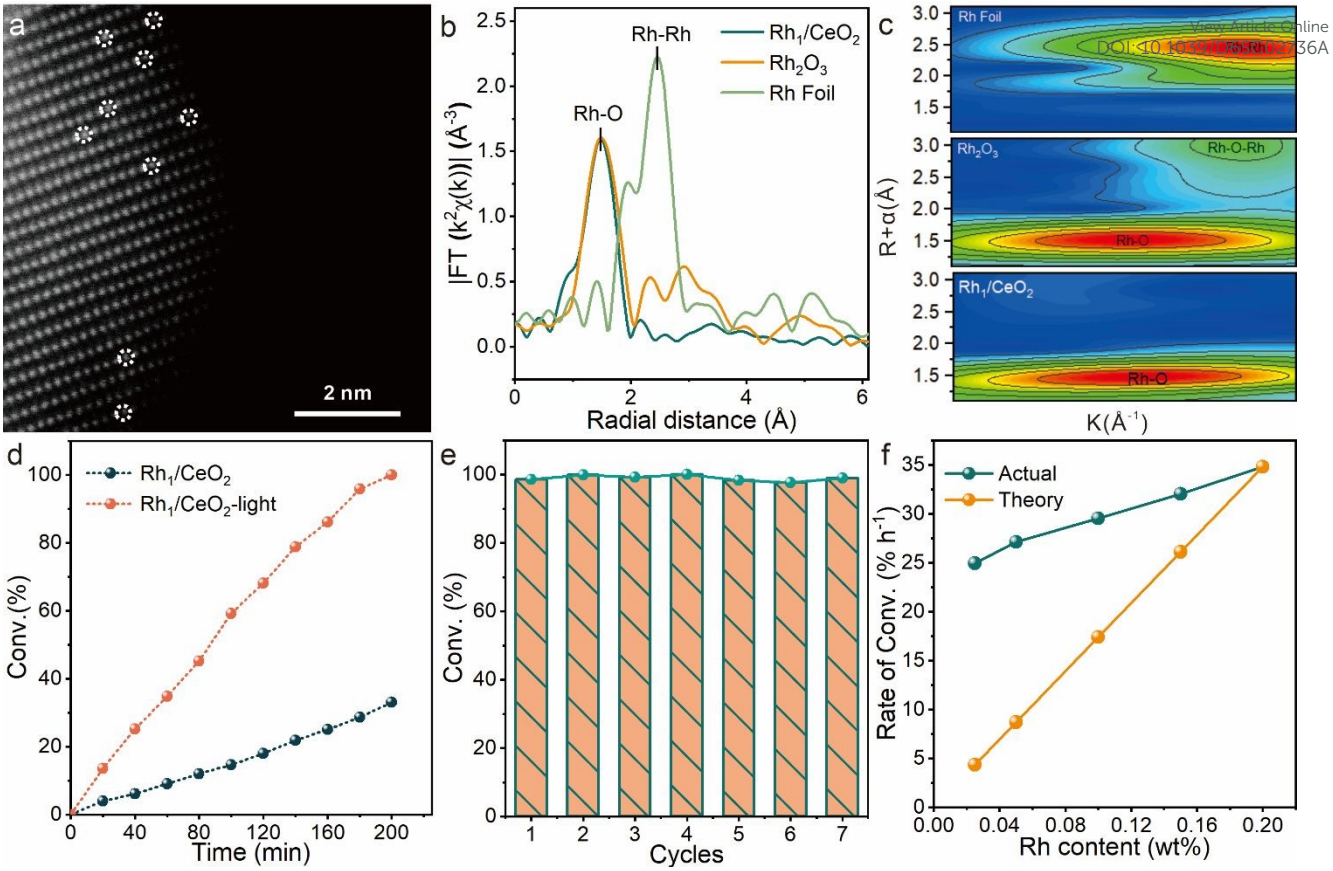


**Figure 1.** (a) A HAADF-STEM image of $Rh_1/CeO_2$ catalyst, (b) Fourier-transform EXAFS spectra of $Rh_1/CeO_2$ and references. (c) The WT-EXAFS spectra of $Rh_1/CeO_2$ and references. (d) Catalytic performance of hydrogenation of styrene on $Rh_1/CeO_2$ under light irradiation. (e) Catalytic durability of $Rh_1/CeO_2$ in the hydrogenation of styrene. (f) The conversion of styrene within 1 h over $Rh_1/CeO_2$ with different loadings of Rh. Reaction conditions: 10 mL $CH_3CN$; 2 μmol Rh; 2 mmol styrene; 303 K; 0.1 MPa $H_2$ or $D_2$; and light source, a 300 W Xenon lamp light (λ> 300 nm)

To further elucidate the mechanism of $H_2$ activation on $Rh_1/CeO_2$, density functional theory (DFT) calculations were performed. As shown in Figure 2a and Figures S14, $H_2$ adsorbed on isolated Rh sites is readily activated via a heterolytic cleavage pathway. In this process, one hydrogen atom migrates to a neighboring oxygen atom to form O-$H^{\delta+}$ species, while the other hydrogen atom remains bound to the Rh center as $H^{\delta-}$. This heterolytic $H_2$ activation step is exothermic by 0.91 eV and proceeds with an activation barrier of 0.36 eV, indicating that hydrogen activation at the Rh-O-Ce interfacial sites is thermodynamically and kinetically favorable. In situ Fourier transform infrared (FT-IR) spectroscopy was subsequently employed to experimentally validate the theoretical predictions (Figure 2b). Upon introduction of $D_2$, a distinct absorption peak emerged at around 2500 $cm^{-1}$, corresponding to the stretching vibration of -OD species. With prolonged $D_2$ exposure, the characteristic -OH stretching peak in the range of 3200-3600 $cm^{-1}$ gradually diminished, while the -OD signal became increasingly pronounced.[35] In contrast, no -OD-related signals were detected for pristine $CeO_2$ under identical $D_2$ treatment conditions (Figure S15). These observations unequivocally demonstrate that the Rh-O-Ce interfacial structure enables heterolytic $H_2$ activation into $H^{\delta-}$ and $H^{\delta+}$ species under mild conditions, whereas $CeO_2$ alone lacks this capability.

To gain further insight into the migration of activated hydrogen species from Rh-O-Ce interfacial sites to FLP sites on $CeO_2$, DFT calculations were conducted to evaluate the hydrogen spillover process. As shown in Figure 2c and Figures S16-S19, the activated hydrogen atoms can readily migrate across the $CeO_2$ surface by overcoming small energy barriers ranging from 0.37-0.58 eV, which are readily accessible under reaction conditions. Experimental evidence for hydrogen spillover was obtained using physical mixtures of $Rh_1/CeO_2$ and $WO_3$ subjected to $H_2$ treatment under light irradiation.[23] As shown in Figure 2d, the $Rh_1/CeO_2$-$WO_3$ mixture exhibits a rapid color change from yellow to dark blue, indicative of hydrogen-induced reduction of $WO_3$ and confirming the migration of activated hydrogen species from $Rh_1/CeO_2$ to $WO_3$. In contrast, this spillover-induced color change is significantly suppressed in the absence of light irradiation or when atomically dispersed Rh atoms are not present (Figure 2d and Figure S20). Furthermore, $H_2$ temperature-programmed reduction ($H_2$-TPR) analysis reveals that the reduction of $CeO_2$ is markedly accelerated by hydrogen spillover originating from Rh-O-Ce interfacial sites (Figure S21). Taken together, these theoretical and experimental results confirm that hydrogen spillover from Rh-O-Ce interfacial sites to FLP sites on $CeO_2$ is both energetically feasible and kinetically accessible, and that light irradiation plays a critical role in facilitating this process

View Article Online
DOI: 10.1039/D6SC00736A

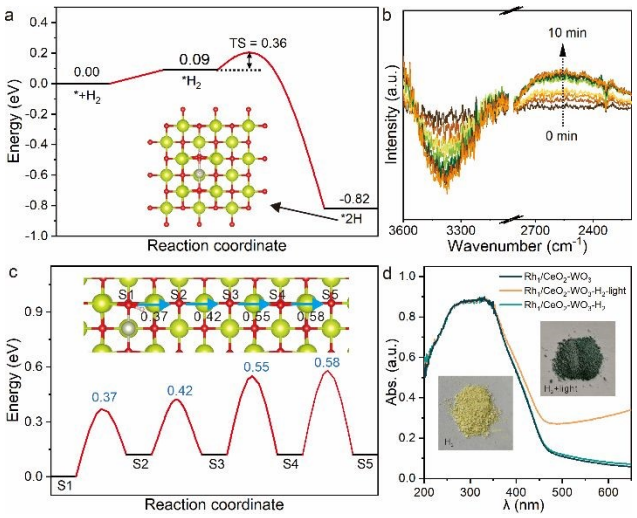


**Figure 2** (a) Energy barriers of transition states and optimized structures of $H_2$ activation on the $Rh_1/CeO_2(100)$ surface. (b) *in-situ* $D_2$-FTIR curves for $Rh_1/CeO_2$. (c) Energy barriers of transition states and optimized structures of the activated H transfer on the $Rh_1/CeO_2(100)$ surface. (d) UV-vis DRS and pictures of physical mixture of $WO_3$ and $CeO_2$ before and after treated with $H_2$ and UV.

Considering that light irradiation can induce the formation of transient FLPs on semiconductor surfaces, we hypothesized that the excellent hydrogenation activity originates from photo-generated transient FLPs serving as the active sites for styrene hydrogenation. To validate this hypothesis, in situ electron paramagnetic resonance (EPR) was employed to monitor changes in the electronic structure under light irradiation. As shown in Figure 3a and Figure S22, upon light irradiation at room temperature, $Rh_1/CeO_2$ exhibits a distinct EPR signal at a g-value of 2.003, which is characteristic of oxygen vacancies formed through the photo-reduction of $CeO_2$. In contrast, no discernible EPR signal is observed in the absence of light irradiation. This comparison confirms that light irradiation induces significant electronic restructuring in $CeO_2$, consistent with previous reports.[36] More importantly, in situ X-ray photoelectron spectroscopy (XPS) reveals that light irradiation leads to the transformation of 22.09% of lattice oxygen ($O_L$) into oxygen-vacancy-associated oxygen species, which act as Lewis acid sites (Figure 3b and Figure S23a). Correspondingly, the Ce(Ⅳ) species adjacent to these oxygen vacancies are partially reduced to Ce(Ⅲ), generating transient Lewis base sites (Figure 3c and Figure S23b). These results collectively provide direct evidence for the photoinduced formation of transient Lewis acid-based pairs on the $CeO_2$ surface.

To directly probe the formation of transient FLPs under light irradiation, $CO_2$ and $NH_3$ are used as molecular probes for Lewis base and Lewis acid sites, respectively. As shown in Figure 3d, $CO_2$ temperature programmed desorption ($CO_2$-TPD) profiles of $Rh_1/CeO_2$ exhibit two desorption peaks in the temperature ranges of 200-300 °C and 300-450 °C, attributable to $CO_2$ adsorption on Lewis base sites associated with oxygen vacancies. Upon light irradiation, while the desorption temperatures remain unchanged, the total amount of desorbed $CO_2$ increases significantly, indicating that light irradiation increases in the number of Lewis base sites without altering their intrinsic absorption strength. Similarly, $NH_3$ adsorption-desorption measurements exhibit analogous behavior (Figure 3e), further confirming that light irradiation enhances the population of Lewis acid sites while preserving their adsorption characteristics.

To further verify that photo-generated transient FLPs serve as the active sites for hydrogenation by spilled hydrogen species, we investigated the relationship between catalytic activity and the density of transient FLPs by introducing additional $CeO_2$ into the reaction system. Specifically, pristine $CeO_2$ is physically mixed with $Rh_1/CeO_2$. As shown in Figure 3f and Figure S24, the hydrogenation activity increases by ~63.82% upon the addition of 0.75 equiv. of $CeO_2$. Moreover, the catalytic activity increases progressively with increasing amounts of added $CeO_2$. These results clearly demonstrate that the spilled hydrogen species participate in hydrogenation reactions at photo-induced transient FLPs sites on $CeO_2$.

To gain deeper insight into the role of spilled hydrogen species in FLP-mediated hydrogenation, DFT calculations were performed to evaluate the Gibbs free energy changes (ΔG) associated with each elementary hydrogenation step. As shown in Figure 3g and Figures S25-S27, the calculated ΔG values for hydrogen addition on FLP sites are strongly negative, indicating that styrene hydrogenation on these sites is thermodynamically favorable. Then, kinetic isotope effect (KIE) measurements and in situ FT-IR analysis were performed to further confirm the involvement of spilled hydrogen species. When $D_2$ was used as the hydrogen source, a pronounced KIE value of 4.43 was observed (Figure 3h), indicative of a primary isotope effect and confirming that proton transfer involving spilled hydrogen species plays a key role in the rate-determining hydrogenation steps. In addition, the signal of –OD on $Rh_1/CeO_2$ gradually disappeared after the introduction of styrene gas, indicating that $D^{\delta+}$ was involved directly in the hydrogenation of styrene (Figure S28). Together, these theoretical and experimental results unambiguously establish that FLP sites on the $CeO_2$ surface serve as the active centers for styrene hydrogenation, in full agreement with the mechanistic insights derived from hydrogen spillover and photo-induced FLP formation.

View Article Online
DOI: 10.1039/D6SC02736A

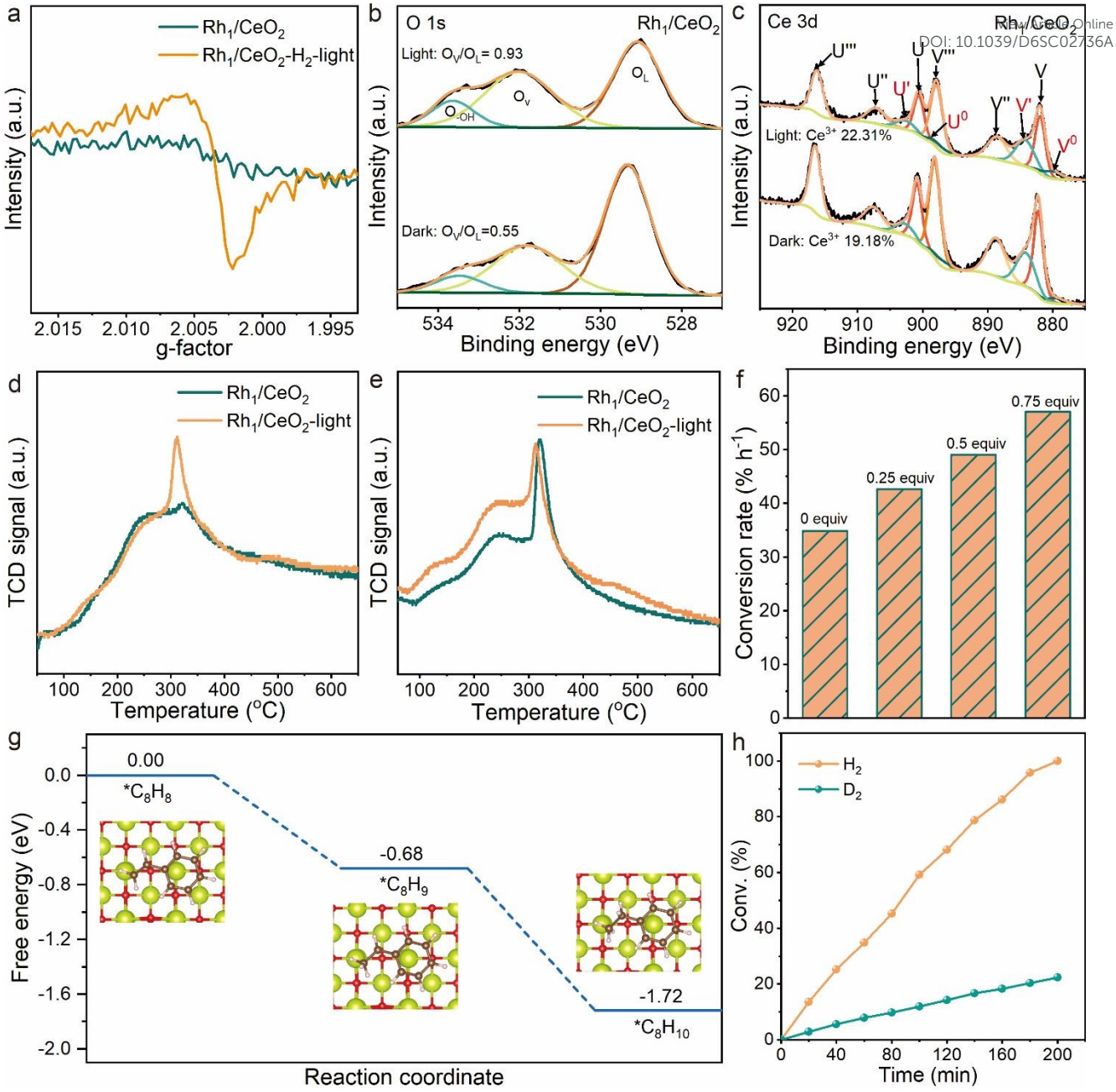


**Figure 3** (a) in-situ EPR curves of $Rh_1/CeO_2$ before and after light irradiation. The XPS binding energy of (b) O 1s and (c) Ce 3d. (d) $CO_2$-TPD and (e) $NH_3$-TPD curves of $Rh_1/CeO_2$ adsorbed $CO_2$/$NH_3$ gas before and after treated with light irradiation ($Rh_1/CeO_2$-light). (f) The reactivity of styrene hydrogenation over the physical mixture of $Rh_1/CeO_2$ and pure $CeO_2$. (g) Stepwise hydrogenation (from 1H to 2H) of styrene. (h) The $H_2/D_2$ isotopic study of styrene hydrogenation catalyzed by $Rh_1/CeO_2$. Reaction conditions: 10 mL $CH_3CN$; 2 μmol Rh; 2 mmol styrene; 303 K; 0.1 MPa $H_2$ or $D_2$; and light source, a 300 W Xenon lamp light (λ> 300 nm).

The above studies collectively demonstrate that photo-induced transient FLPs generated under light irradiation are essential for achieving the enhanced hydrogenation activity. We thus expect that the photo enhanced catalytic hydrogenation should promote the hydrogenation of a wide range of unsaturated compounds. Experimentally, $Rh_1/CeO_2$ also displays excellent catalytic performance in the hydrogenation of other unsaturated compounds, such as 4-tert-butylstyrene, 4-chlorostyrene, nitrobenzene, 4-chloronitrobenzene, diketene, and allylacetone, with activities of 26.4%//h, 58.0%/h, 59.4%/h, 53.1%/h, 40.9%/h, and 70.2%/h, (Figure 4a and Figure S30) respectively. Based on this understanding, we further sought to extend this concept to other semiconductor-supported, isolated Rh catalysts to establish the universal principles of photo-driven transient FLPs for catalytic hydrogenation. Following a similar synthetic strategy used for $Rh_1/CeO_2$, isolated metal atoms were deposited onto a series of semiconductor supports, including $TiO_2$, ZnO, $LaTiO_2N$, $SrTaO_2N$, via reductive deposition and subsequent deposition-precipitation methods (Figures S30-S33). The hydrogenation performance of the resulting catalysts was evaluated using styrene as a probe substrate. As shown in Figure 4b and Figure

S34, all semiconductor-supported catalysts exhibit markedly enhanced hydrogenation activity toward the alkene products compared with the corresponding metal-on-carbon reference catalyst under identical conditions. These results demonstrate that the synergistic interplay between isolated metal sites—responsible for efficient $H_2$ activation—and photo-driven transient FLPs—serving as hydrogenation centers—is a general and effective strategy for turning catalytically inert semiconductor supports into highly active hydrogenation catalysts under mild reaction conditions.

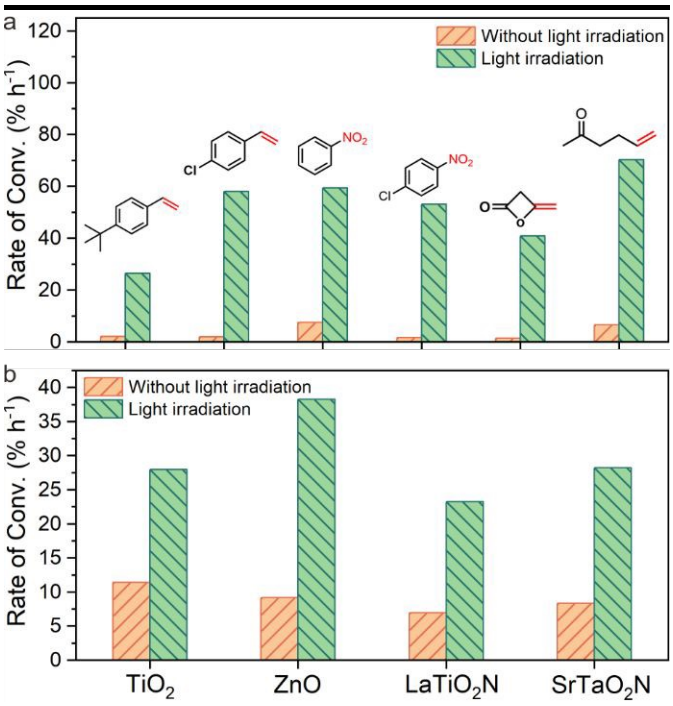


**Figure 4.** (a) Conversion rates of photocatalytic other unsaturated compounds hydrogenation over $Rh_1/CeO_2$. (b) Conversion rates of $TiO_2$, ZnO, $LaTiO_2N$ and $SrTaO_2N$. Reaction conditions: 10 mL $CH_3CN$; 2 μmol Rh; 2 mmol styrene; 303 K; 0.1 MPa $H_2$ or $D_2$; and light source, a 300 W Xenon lamp light (λ> 300 nm).

## Conclusions

In summary, this work demonstrates a synergistic strategy to overcome the intrinsic limitations of heterogeneous frustrated Lewis pairs (FLPs) for catalytic hydrogenation under mild conditions. By anchoring isolated Rh species onto $CeO_2$, well-defined Rh-O-Ce interfacial sites are constructed that enable efficient heterolytic $H_2$ activation into Rh-$H^{\delta-}$ and O-$H^{\delta+}$ species. Under light irradiation, the hydrogen spillover process from these interfacial sites to FLP sites on the oxide surface is markedly promoted, while photoexcitation of $CeO_2$ simultaneously generates abundant transient FLPs. The cooperative interplay between photo-enhanced hydrogen spillover and photo-induced FLP formation results in substantial enhancement in photocatalytic hydrogenation activity, exemplified by the markedly improved hydrogenation rate of a wide range of unsaturated compounds compared with pristine $CeO_2$. Importantly, the observation of similar synergistic effects on other semiconductor supports highlights the general applicability of this approach. This study establishes a versatile dual-active-site design principle that integrates interfacial metal-oxide sites with photoinduced FLPs, providing a new and broadly applicable pathway for the rational design of efficient photocatalytic hydrogenation systems.

View Article Online
DOI: 10.1039/D6SC02736A

## Author contributions

**Jin Lin:** Writing – original draft, Data curation, Investigation; **Shuanghui Chen:** Data curation, Investigation; **Kang-Shun Peng:** Investigation; **Yung-Hsi Hsu:** Investigation; **Shuchun Li:** Investigation; **Longji Cui:** Investigation; **Hansong Zhang:** Investigation; **Yongjie Wang:** Investigation; **Xue Feng Lu:** Investigation; **Sibo Wang:** Investigation; **Kunlong Liu:** Writing – review & editing, Project administration, Supervision, Funding acquisition; **Sung-Fu Hung:** Resources, Writing – review & editing, Supervision; **Xinchen Wang:** Writing – review & editing, Project administration, Supervision, Funding acquisition.

## Conflicts of interest

There are no conflicts to declare.

## Data availability

The data supporting this article have been included as part of the supplementary information (SI). Supplementary information is available.

## Acknowledgements

This work was financially supported by the National Natural Science Foundation of China (22302040, U24A20567, 22572034, and 22032002), 111 Project (D16008), and Fujian Provincial Natural Science Foundation of China (2026J001096). The supports from the National Science and Technology Council, Taiwan (Contract No. NSTC 114-2628-M-A49-005) are gratefully acknowledged. We also thank the support from the Yushan Young Scholar Program (MOE 114-YSFMS-0010-003-P2) and the Center for Emergent Functional Matter Science, Ministry of Education, Taiwan. The authors acknowledged the facility resources from Electron Microscopy Center of Fuzhou University. The authors are grateful to Dr. Liangping Xiao for her help with the analysis of TEM results in this paper. We would like to thank the reviewers for their helpful remarks.

## References

1. W. Jia, H. Wang, C. Xue, Y. Li and Q. Xiao, ACS Applied Nano Materials, 2025, 8, 11095-11103.
2. J. Li and Y. Shi, Chemical Society Reviews, 2022, 51, 6757-6773.
3. Y. Li, K. Yan, Y. Cao, X. Ge, X. Zhou, W. Yuan, D. Chen and X. Duan, ACS Catalysis, 2022, 12, 12138-12161.

4. A. Primo, F. Neatu, M. Florea, V. Parvulescu and H. Garcia, Nature Communications, 2014, 5, 5291.
5. L. Zhong, X. Liao, H. Huang, H. Cui, J. Huang, H. a. Luo, Y. Pei, Y. Lv and P. Liu, Journal of the American Chemical Society, 2025, 147, 3840-3854.
6. Z. Tian, L. Wang, T. Shen, P. Yin, W. Da, Z. Qian, X. Zhao, G. Wang, Y. Yang and M. Wei, Chemical Engineering Journal, 2023, 472, 144876.
7. Y. Ma, S. Zhang, C.-R. Chang, Z.-Q. Huang, J. C. Ho and Y. Qu, Chemical Society Reviews, 2018, 47, 5541-5553.
8. Z.-Q. Huang, L.-P. Liu, S. Qi, S. Zhang, Y. Qu and C.-R. Chang, ACS Catalysis, 2018, 8, 546-554.
9. S. Zhang, Z.-Q. Huang, Y. Ma, W. Gao, J. Li, F. Cao, L. Li, C.-R. Chang and Y. Qu, Nature Communications, 2017, 8, 15266.
10. V. Muravev, A. Parastaev, Y. Van Den Bosch, B. Ligt, N. Claes, S. Bals, N. Kosinov and E. J. M. Hensen, Science, 2023, 380, 1174-1179.
11. Z. Wang, X. Yuan, H. Guo, X. Zhang, J. Peng and Y. Pan, Energy & Environmental Science, 2024, 17, 8019-8056.
12. F. Kong, X. Lu, J. Xie, Z. Lu, J. Hu and Y. Cao, Inorganic Chemistry Frontiers, 2024, 11, 2932-2944.
13. X. Gao, L. Li, Z. Zhao, Y. J. Dappe, Z.-J. Jiang, P. Song, Y. Wang and J. Zhu, Applied Catalysis B: Environment and Energy, 2025, 364, 124835.
14. W. Jiang, H. Loh, B. Q. L. Low, H. Zhu, J. Low, J. Z. X. Heng, K. Y. Tang, Z. Li, X. J. Loh, E. Ye and Y. Xiong, Applied Catalysis B: Environmental, 2023, 321, 122079.
15. C. Chu, D. Huang, S. Gupta, S. Weon, J. Niu, E. Stavitski, C. Muhich and J.-H. Kim, Nature Communications, 2021, 12, 5179 (2021)
16. Q. Wang, D. Zhang, Y. Chen, W.-F. Fu and X.-J. Lv, ACS Sustainable Chemistry & Engineering, 2019, 7, 6430-6443.
17. S. Wang, X. Hai, X. Ding, K. Chang, Y. Xiang, X. Meng, Z. Yang, H. Chen and J. Ye, Advanced Materials, 2017, 29, 1701774.
18. Q. Ren, Y. He, H. Wang, Y. Sun and F. Dong, ACS Catalysis, 2022, 12, 14015-14025.
19. T. Xu, J. Shi, K. S. Peng, Y. H. Hsu, Y. C. Liu, S. Wang, H. Zhang, Y. Wang, G. Zhang, S. F. Hung, K. Liu and X. Wang, Angewandte Chemie International Edition, 2025, 64, e202513029.
20. Z. Yuan, L. Huang, Y. Liu, Y. Sun, G. Wang, X. Li, J. A. Lercher and Z. Zhang, Angewandte Chemie International Edition, 2024, 63, e202317339.
21. Z. Tian, L. Wang, T. Shen, P. Yin, W. Da, Z. Qian, X. Zhao, G. Wang, Y. Yang and M. Wei, Chemical Engineering Journal, 2023, 472.
22. Y. Liang, Z. Zhang, X. Su, X. Feng, S. Xing, W. Liu, R. Huang and Y. Liu, Angewandte Chemie International Edition, 2023, 62, e202309030.
23. J. Cui, T. Yang, T. Xu, J. Lin, K. Liu and P. Liu, Chinese Journal of Structural Chemistry, 2025, 44, 100438.
24. H. Dai, A. Wu, A. Zhang, W. Chen and C. Zhou, Applied Surface Science, 2025, 687, 162288.
25. Y. Zhang, S. Zhan, K. Liu, M. Qiao, N. Liu, R. Qin, L. Xiao, P. You, W. Jing and N. Zheng, Angewandte Chemie International Edition, 2023, 62, e202217191.
26. R. Liu, Y. Shi, L. Lin, Z. Wang, C. Liu, J. Bi, Y. Hou, S. Lin and L. Wu, Applied Surface Science, 2022, 605.
27. J. Wang, H. Zhao, B. Zhu, S. Larter, S. Cao, J. Yu, M. G. Kibria and J. Hu, ACS Catalysis, 2021, 11, 12170-12178.
28. L. Zhang, R. Li, L. Guo, L. Cui, X. Zhang, Y. Wang, Y. Wang, X. Jian, X. Gao, C. Fan, J. Wang and J. Liu, ACS Catalysis, 2024, 14, 5696-5709.
29. L. Jiang, K. Liu, S.-F. Hung, L. Zhou, R. Qin, Q. Zhang, P. Liu, L. Gu, H. M. Chen, G. Fu and N. Zheng, Nature Nanotechnology, 2020, 15, 848-853.
30. L. Zhou, L. Zhuo, R. Yuan and G. Fu, WIREs Computational Molecular Science, 2021, 11, e1531.
31. P. Liu, R. Qin, G. Fu and N. Zheng, Journal of the American Chemical Society, 2017, 139, 2122-2131.
32. S. Wang, L. Zhao, W. Wang, Y. Zhao, G. Zhang, X. Ma and J. Gong, Nanoscale, 2013, 5, 5582.
33. R. Qin, L. Zhou, P. Liu, Y. Gong, K. Liu, C. Xu, Y. Zhao, L. Gu, G. Fu and N. Zheng, Nature Catalysis, 2020, 3, 703-709.
34. J. Xu, Y. Wang, K. Wang, M. Zhao, R. Zhang, W. Cui, L. Liu, M. S. Bootharaju, J. H. Kim, T. Hyeon, H. Zhang, Y. Wang, S. Song and X. Wang, Angewandte Chemie International Edition, 2023, 62, e202302877.
35. D. Panayotov, E. Ivanova, M. Mihaylov, K. Chakarova, T. Spassov and K. Hadjiivanov, Physical Chemistry Chemical Physics, 2015, 17, 20563-20573.
36. X. Huang, K. Zhang, B. Peng, G. Wang, M. Muhler and F. Wang, ACS Catalysis, 2021, 11, 9618-9678.

View Article Online
DOI: 10.1039/D6SC02736A

## Data Availability Statement

The data supporting this article have been included as part of the supplementary information (SI). Supplementary information is available.